VIROLOGY 213, 341–351 (1995)

MANFRED J. SCHMITT[1] and DONALD J. TIPPER*

*Institut für Mikrobiologie und Weinforschung, Johannes Gutenberg-Universität Mainz, D-55099 Mainz, Germany; and *Department of Molecular Genetics and Microbiology, University of Massachusetts Medical School, Worcester, Massachusetts 01655*

Received May 22, 1995; accepted July 17, 1995

The killer and immunity phenotypes of K28 killer strains of *Saccharomyces cerevisiae* are determined by the 1.75-kb M28 dsRNA virus. In the plus strand, M28p, the K28 preprotoxin gene, comprises bases 13–1047 and is followed, after an additional 85 bases, by a 63-bp poly(A) sequence and a 553-base 3′-sequence. This 3′-sequence contains two potential stem–loop structures predicted to bind the L-A encoded cap–pol protein, initiating encapsidation; high-level expression results in curing of M1 dsRNA. Expression of M28p confers the complete K28 killer and immunity phenotype on a cell lacking M28 dsRNA. K28 toxin is a disulfide-bonded heterodimer of α (10.5 kDa) and β (11 kDa) components whose N-termini correspond to M28p residues 50–61 and 246–257, respectively. α is preceded by a potentially redundant pair of secretion signal peptides; deletion of the first reduces toxin secretion by 75%. While M28p bears no sequence similarity to M1p, the K1 preprotoxin, the predicted patterns of processing by glycosylation and cleavage are remarkably similar. The β N- and C-termini are probably processed by Kex2p and Kex1p, respectively; the mechanism of cleavage at the less typical sites bounding the α component is under investigation. While a *kex2*Δ mutation prevents toxin secretion, secreted toxin retains 20% activity in a *kex1*Δ mutant. Neither mutation affects immunity.

INTRODUCTION

Killer strains of the yeast *Saccharomyces cerevisiae* secrete protein toxins that kill sensitive cells of the same and related yeast species. Such killers are resistant to their own toxin and killers are classified according to this specific resistance pattern which is called immunity (Tipper and Schmitt, 1991; Wickner, 1992). The majority of natural *S. cerevisiae* isolates are sensitive nonkillers. Among the killer types identified in *S. cerevisiae,* only three, K1, K2, and K28, have been studied in any detail. These killers produce K1, K2, and K28 toxins and each kills members of the other types (Schmitt and Tipper, 1990). The K1 and K2 toxins cause membranes of sensitive cells to become leaky, while the first observable effect of K28 toxin is inhibition of DNA synthesis (Schmitt *et al.,* 1989; Bussey, 1991). The mechanisms of toxin action and immunity are unknown. Killing requires initial binding of the toxin to a cell wall component, a β-1,6-glucan component for K1 and K2 toxins (Bussey, 1991), and an α-1,3-mannan component for K28 toxin (Schmitt and Radler, 1987). A sensitive strain can become resistant by a *kre* mutation that modifies this cell wall receptor. Protoplasts of such mutants, however, remain sensitive. Immune, toxin-producing cells have normal cell wall receptors but resistant spheroplasts, implying the existence of a secondary membrane receptor (Tipper and Schmitt, 1991).

[1] To whom correspondence and reprint requests should be addressed. Fax: (49) 6131 392695.

The K1, K2, and K28 toxin and immunity phenotypes are encoded by cytoplasmic dsRNA viruses with genomes of about 1.8 kb called M1, M2, and M28, respectively (Tipper and Schmitt, 1991). These viruses are satellites of L-A, a 4.6-kb dsRNA virus that encodes the capsid and cap–pol components of the virions encapsidating both L and M dsRNA species (Wickner, 1993). Strains containing only L-A or no dsRNA are sensitive unless they carry a *kre* mutation. The cap–pol fusion protein is produced by a −1 frameshift, occurring at a frequency of about 2% during translation of the L-A plus-strand transcript (Dinman and Wickner, 1992, 1994). The cap–pol components in each virion are responsible for production of these transcripts which are released into the cytoplasm and translated in a cap-independent fashion. When concentration of the cap-pol translation product is sufficiently high, it binds to a stem–loop structure in its own L-A plus-strand messenger or the M plus-strand transcript, initiating encapsidation (Fujimura *et al.,* 1990). The polymerase component then initiates minus-strand synthesis at the plus-strand 3′-termini, completing viral replication (Wickner, 1993).

L-A and M dsRNA sequences have been deduced from analyses of dsRNA terminal sequences and of cDNAs derived using denatured dsRNA or plus-strand transcripts as template. Complete sequences have been published only for L-A (Icho and Wickner, 1989) and for the various fragments of M1 (Bostian *et al.,* 1984; Georgopoulos *et al.,* 1986; Skipper, 1983). The published sequence for M2 covers the open reading frame (ORF)

0042-6822/95 $12.00

(Dignard *et al.,* 1991). We now describe the complete sequence of M28. Comparisons emphasize the conserved pattern of functional elements in M1 and M28 and reinforce models for the sequence elements required for viral replication.

The ORFs in M1, M2, and M28 (Schmitt, 1995) comprise 316, 362, and 345 codons and initiate with AUG at bases 14, 7, and 13 of the plus strand, respectively. The deduced primary translation products are called K1, K2, and K28 preprotoxins, M1p, M2p, and M28p, respectively. Each initiates with a potential secretion signal, consistent with function as a precursor of a secreted toxin. Expression of a cDNA copy of the K1 or K2 reading frame in a sensitive yeast strain leads to expression of the complete toxin secretion and immunity phenotype of the parent dsRNA (Dignard *et al.,* 1991; Hanes *et al.,* 1986; Lolle *et al.,* 1984). We have recently shown that this is also true for a cDNA covering all but the first three codons of the K28 preprotoxin gene (Schmitt, 1995). Translation presumably initiated at the first AUG, codon 15 of the complete preprotoxin. We now show that initiation at the normal AUG enhances expression fourfold. Hydropathy analysis of the M28p N-terminus suggests redundancy in secretion signal function, consistent with this flexibility in translational initiation site.

The preprotoxins bear no sequence relationship to each other or to other known proteins. They do, however, share conserved patterns of potential processing sites. Each preprotoxin has three sites for N-glycosylation, so that, following signal cleavage, a core-glycosylated protoxin should be secreted into the lumen of the endoplasmic reticulum. This has, so far, been demonstrated only for the K1 toxin precursor (Bostian *et al.,* 1983). The mature K1 toxin comprises two disulfide-bonded species, α and β, of 9 and 9.5 kDa (Bostian *et al.,* 1984). N-terminal sequence analysis indicates that processing of these toxin fragments from M1p closely resembles insulin processing (Bostian *et al.,* 1984). Published data on the K2 toxin are insufficient for comparison (Dignard *et al.,* 1991).

Mutations in two killer expression genes, *KEX1* and *KEX2,* prevent or reduce secretion of K1 and K2 toxins without affecting immunity (Wickner and Leibowitz, 1976). The product of the *KEX2* gene, Kex2p, is a transmembrane, subtilisin-like protease, autocatalytically activated and localized in a late Golgi compartment with its active site in the lumen (Brenner and Fuller, 1992). It is the prototype for furin and the expanding family of processing endopeptidases now known to be required for maturation of metazoan peptide hormones (Steiner *et al.,* 1992). It cleaves preferentially after LysArg or ArgArg pairs of basic residues (Brenner and Fuller, 1992) and has also been shown to be required for production of the N-terminus of the K1 α toxin component by cleavage after ProArg (Zhu *et al.,* 1992). Kex1p is a carboxypeptidase that removes the basic residues exposed by the action of Kex2p (Cooper and Bussey, 1989; Dmochowska *et al.,* 1987). We now show that K28 toxin, like K1 toxin, comprises two disulfide-bonded fragments. While Kex2p activity is absolutely required for their production, a *kex1* null mutation reduces secreted activity by only 80%. The deduced pattern of K28 protoxin processing is remarkably similar to that of M1p, although some predicted processing sites fall outside of the recognized Kex2p specificity. Implications for processing of secreted proteins are discussed.

MATERIALS AND METHODS

Yeast strains and media

Genotypes and dsRNA contents of all *S. cerevisiae* strains used in this work are listed in Table 1. *Escherichia coli* strains JM105, JM109, and DH5α were used for maintenance and production of plasmid DNAs. YEPD medium, methylene blue agar (MBA) for testing killer phenotype, and minimal media have previously been described (Schmitt and Tipper, 1990; Schmitt and Radler, 1987; Schmitt and Pfeiffer, 1990). Yeast strains were cured of their killer phenotype by cultivation in YEPD medium either at elevated temperature (38°) or in the presence of cycloheximide (up to 1 μg/ml), as previously described (Schmitt and Tipper, 1992).

Plasmids

Plasmids pMS12, pMS19, and pMS33 have been previously described (Schmitt, 1995). Plasmids YEpDT-PGK, p21-PGK-SPB, and p21-GAL1-SPB have also been previously described (Cartwright *et al.,* 1994; Kang *et al.,* 1990). The complete M28p reading frame was cloned by PCR using pMS19 as template. The first primer, ODT164, (5′) GGGGAATTCTCGAGACC ATG G/AAG AGC GTT TCC TCT TTA TTT AAC ATT, provided the missing three N-terminal codons (in boldface) preceded by an *Xho*I site. The second codon is either Glu (wild type) or Lys; the two products are distinguished by the *Nco*I site in the former. The second primer, ODT165, (5′) GGGAGATCTA TTA GCG TAG CTC ATC GTG, is complementary to the C-terminus of the ORF and is immediately followed by a *Bgl*II site. The product was cloned as an *Xho*I to *Bgl*II fragment into p21-PGK-SPB cut with *Xho*I and *Bgl*II to eliminate the SPB fragment that lies between the *PGK* promoter and terminator fragments. The product, pDT-P-M28, differs from pMS33 only in the cDNA insert in this expression site. Replacement of the *PGK* promoter fragment in pDT-P-M28 with the *GAL1* promoter fragment from p21-GAL1-SPB (Cartwright *et al.,* 1994) produced pDT-G-M28. The 693-bp M28b fragment of M28 dsRNA downstream of the M28p gene was cloned by PCR using pMS19 as template. The first primer, ODT206, (5′) GGG-CTCGAG CCAGACCGA CGCTTCTT, starts at M28 base 1055 preceded by an *Xho*I site. The second primer, ODT207, (5′) GGGCTGCAG TGTTATG AGGCAAAGTA TTTTGTTAGT TAACTAGTATC, is the complement of the

TABLE 1

S. cereviaiae Strains Used in This Study

Strain	Genotype	dsRNA	Reference
28	Unknown	L-A_{28} M_{28}	Pfeiffer and Radler, 1984
28c	Unknown	L-A_{28} M-0, cycloheximide-cured	Schmitt and Tipper, 1990
381	Unknown, prototrophic diploid	L-A L-B	Schmitt and Tipper, 1990
MS205	MATa Ura3-2 Leu2 His3	L-A L-B M_{28}	This study
S86c	MATα Ura3-2 Leu2 His3 Pra1 Prb2 Prc1 Cps1	L M-0	Cooper and Bussey, 1989
S86-1c	MATα Ura3-2 Leu2 His3 Pra1 Prb2 Prc1 Cps1 Kex1::LEU2	L M-0	Cooper and Bussey, 1989
GG100-14D	MATα Ura3-52 His3 Trp1 Pho3 Pho5	L-A L-B M-0	Bostian *et al.,* 1983
GGMS1	K1 killer produced by M1 transfection of GG100-14D		Sturley *et al.,* 1986
ME938	MATα Bar1 Leu2-3, 112 Ura3 Gal2 Kex2::Ura3 Yap3::LEU2		Egel *et al.,* 1990
MT960	MATα Bar1 Leu2-3, 112 Ura3 Gal2		Egel *et al.,* 1990
CRY1	MATa Ura3-1 Leu2-3 112 Trp1-1 His3-11 Ade2-1^{oc} Can1-100		Zhang *et al.,* 1994
BFY126-35a	Kex2::HIS3 derivative of CRY1		Zhang *et al.,* 1994

plus-strand 3′-terminus, including the missing 16 bases (in boldface), followed by a *Pst*I site. The product, cut with *Xho*I and *Pst*I, was cloned into p21-GAL1-SPB cut with the same enzymes to produce pDT-G-M28b; the M28b fragment, followed by the terminal 385 bp of the β-lactamase gene, is inserted between the *GAL1* promoter and the *PGK* terminator.

Genetic techniques

Mating and virus transfection experiments were performed as previously described (Schmitt, 1995; Schmitt and Tipper, 1992). dsRNAs were prepared by a rapid procedure from cells grown to stationary phase in YEPD medium and analyzed by electrophoresis in 1% agarose gels as previously described (Schmitt and Tipper, 1992). Yeast cells were transformed by the lithium acetate method (Gietz and Schiestl, 1991) and selected by plating on uracil-deficient minimal medium (SC-Ura). dsDNA sequencing (Sanger *et al.,* 1977) was performed using Sequenase 2.0 (United States Biochemical) and α-^{35}S-dATP. The complete cDNA sequence was determined by primer walking.

Killer assay

The K28 killer phenotype was determined by replica plating or patching colonies of killer strains onto MBA plates (pH 4.7) that had been seeded with an overlay of 10^5 cells of the sensitive *S. cerevisiae* strain 381. After 72 hr at 20°, killer activities could be observed as clear zones of growth inhibition surrounding test colonies. For quantitation of K28 toxin, meiotic segregants were grown in YEPD–citrate, pH 4.7, medium (Schmitt and Radler, 1987) and transformants were grown in SC-Ura, pH 4.7, to early postexponential phase (5×10^7 cells/ml). Aliquots (100 μl) of culture supernatants were transferred to wells (10-mm diameter) cut in MBA plates seeded with strain 381. Diameters of zones of growth inhibition were determined after 72 hr at 20°. Toxin concentration is proportional to the log of diameter and is expressed in arbitrary units: 1 U corresponds to 0.1 ng of purified toxin (Schmitt and Radler, 1989).

K28 toxin preparation and purification

Crude toxin was prepared by concentration of the culture supernatant of the wild-type killer strain 28 as previously described (Schmitt and Radler, 1987; Pfeiffer and Radler, 1984). Toxin was partially purified either by ion-exchange chromatography on S-Sepharose or by receptor-mediated affinity chromatography on mannoprotein–CNBr–Sepharose (Schmitt and Radler, 1989). Toxin samples were dialyzed against water, lyophilized, dissolved in sample buffer (50 μl), and fractionated by SDS–PAGE (Laemmli, 1970), with and without reducing agent, using 15% or 5 to 22% gradient gels followed by detection with Coomassie blue. Size markers were the low-molecular-weight markers from Pharmacia or Boehringer-Mannheim.

Protein sequencing

Toxin fractionated by SDS–PAGE was electroblotted onto polyvinylidene difluoride membranes using 10 m*M* CAPS buffer, pH 11, in 10% methanol as described (Matsudaria, 1987). N-terminal sequence analysis by Edman degradation was performed using an Applied Biosystems 477-A sequencer with Model 12-A HPLC and 900A data reduction module.

RESULTS

The complete sequence of M28 dsRNA

We recently reported the construction and expression of a nearly complete cDNA copy of M28 dsRNA (Schmitt, 1995). Primers used for first-strand cDNA synthesis were based on 3′-terminal sequences determined for the separated dsRNA minus and plus strands. Using these plus and minus strands as templates and *Eco*RI/*Not*I adapters, cDNA products of 1.1 and 1.6 kb were cloned into the *Eco*RI site of pUC19. Recombination using the *Cla*I

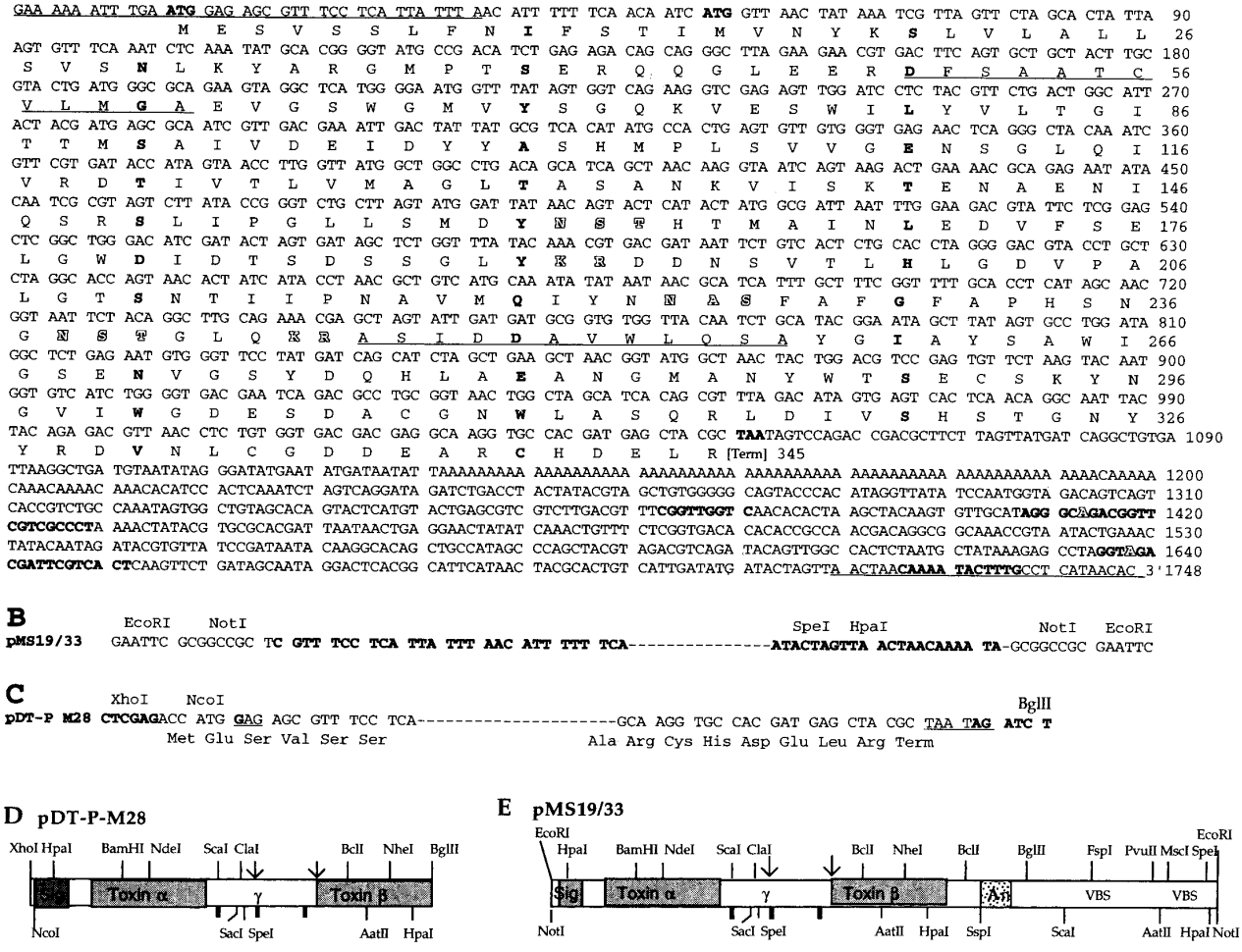

FIG. 1. Sequence of M28 dsRNA and derived cDNA clones. (A) Sequence for the M28 dsRNA plus strand. Terminal sequences determined by analysis of the dsRNA are underlined. Bases 21–1732 were determined from the cDNA clone fragments in pMS19. The potential methionine initiation codons at bases 13–15 and 55–57 and the termination codon at 1047–1050 in the M28p preprotoxin open reading frame are shown in boldface. This open reading frame is shown in single-letter code with every 10th residue in boldface. The N-terminal sequences determined for the mature α and β toxin components, initiating at codons 50 and 246, respectively, are underlined. Potential Kex2 processing sites at KR_{192} and KR_{245} and the N-glycosylation sites at $N_{161}ST$, $N_{224}AS$, and $N_{238}ST$ are shown in the outline font. The potential VBS sequences centered at 1419 and 1644 and the possible 3′ terminal element centered at 1731 are also indicated in boldface. The bulged As are in an outline font. (B) Terminal sequences for the cDNA fragment in pMS19 and pMS33, shown from the *Eco*RI sites of the adapters used in cloning. cDNA bases, shown in boldface, correspond to dsRNA bases 21–1732. (C) The ends of the M28p open reading frame constructed by PCR in pDT-P-M28. The complete N-terminal signal initiates at the *Nco*I site and the β toxin component is assumed to terminate at the *Bgl*II site. (D) Restriction and physical map of the reconstructed complete M28p ORF in pDT-P-M28. The signal and mature α and β toxin components are shown in gray; the probable positions of their C-termini are discussed in the text. The presumed sites of N-glycosylation and Kex2p processing are indicated by vertical bars and arrows, respectively. (E) Restriction map of the cDNA inserts in pMS19 and pMS33. Except for the truncated secretion signal, M28p components correspond to those shown in D. The approximate locations of the poly(A) and VBS sequences downstream of the M28p ORF are indicated.

site shared by the two cDNA clones produced pMS19 with an *Eco*RI fragment insert of approximately 1.7 kb. pMS19 hybridized weakly to both primers, demonstrating at least partial overlap with both RNA terminal sequences.

The complete sequence of the M28 dsRNA plus strand is shown in Fig. 1A. The sequences determined for the dsRNA termini are underlined. Bases 21–1732 are derived from the sequence of the cDNA in pMS19, whose termini are shown in Fig. 1B and whose restriction map is shown in Fig. 1E. The cDNA lacks 20 bases of the plus-strand 5′-terminus and 16 bp from the 3′-terminus, consistent with the relatively weak hybridization signals seen with either primer. The deduced length of M28 dsRNA is 1748 bp. The 345-codon open reading frame presumed to correspond to M28p comprises bases 13–1047. The cDNA sequence includes a 63-bp internal poly(A) sequence (bases 1132–1195), 85 bp downstream from the M28p open reading frame. The residual 553-bp 3′-terminal sequence is presumed to provide the structural elements required for RNA replication. Apart from M28p and discounting the internal poly(A) stretch, the only open reading frame of significant length in M28 dsRNA is of 55 codons on the minus (antisense) strand

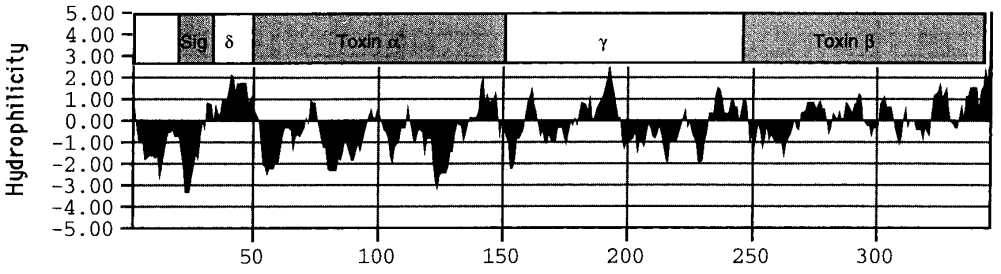

FIG. 2. Hydrophilicity analysis of M28p using the Kyte–Doolittle algorithm with a window size of 7. The indicated preprotoxin fragments correspond to those shown in Fig. 1D.

from bases 668 to 504. It is unlikely to be of significance, since the minus strand is never normally free in the cytoplasm (Wickner, 1993).

Low-stringency Southern blotting, using labeled M28 cDNA probes, failed to detect any chromosomal homolog in *S. cerevisiae* DNA (not shown). Similar results were previously found using the M1 cDNA as probe (Bostian *et al.,* 1984).

Expression of M28p: Predicted cleavage by signal peptidase

The first AUG initiation codon of the M28 plus strand is found at bases 13–15, in frame with the downstream M28p open reading frame. Since translation of yeast mRNAs normally initiates at the first AUG codon, this is presumably the first codon of M28p. The predicted size of M28p (37.64 kDa) agrees with the 38 kDa observed for the *in vitro* translation product of M28 plus-strand RNA (Schmitt, 1995). Additional in-frame AUG codons are found at codons 15 and 37.

Insertion of the *Eco*RI fragment from pMS19 between the *PGK* promoter and terminator fragments of the YEp expression vector pDT-PGK produced pMS33. A sensitive yeast strain transformed with pMS33 expressed the complete K28 killer and immunity phenotypes (Schmitt, 1995). Since pMS33 lacks the first three codons of M28 dsRNA, translation presumably initiated at codon 15. Hydropathy analysis of M28p (Fig. 2) shows the N-terminus to contain two consecutive hydrophobic stretches, at 4–16 and 21–28. A plot of signal peptidase cleavage probability (Fig. 3), following the rules codified by von Heijne (1986), suggests that the context of both hydrophobic stretches is consistent with secretion signal function, cleavage occurring either after Ala_{24} or after Leu_{31}, with the latter being most probable, even though this would produce a protoxin initiating with lysine, an uncommon N-terminus (von Heijne, 1986). Cleavage at this site would be consistent with active expression from pMS33, since the first 14 residues of M28p are probably not essential for signal function.

To test the effect of the missing residues on the efficiency of toxin secretion, a complete copy of the M28p open reading frame was cloned by PCR as a 1048-bp *Xho*I to *Bgl*II fragment using pMS19 as template. The product was cloned between the *PGK* promoter and terminator fragments of the YEp expression vector p21-PGK-SPB (Cartwright *et al.,* 1994), a derivative of YEpDT-PGK (Kang *et al.,* 1990), producing pDT-P-M28. As shown in Fig. 1C, the product includes all 345 codons of M28p with the *Xho*I site at base −9 and the *Bgl*II site immediately downstream of the termination codon. The restriction map is shown in Fig. 1D. pDT-P-M28 differs from pMS33 only at the N-terminus of M28p and in lacking the 693 bases downstream of the M28p termination codon. In transformants of sensitive strains S86c, GG100-14d, or CRY1, the complete K28 killer (Fig. 4) and immunity phenotypes were expressed. Toxin production was about fourfold higher than from pMS33, although mRNA levels were similar (data not shown). The increase pre-

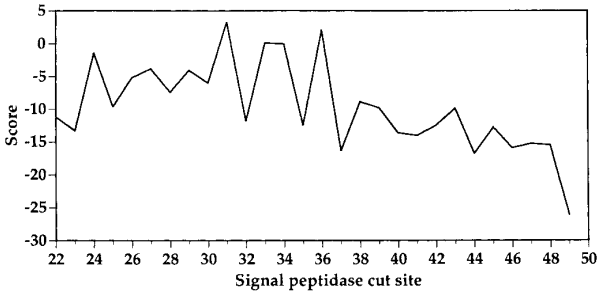

FIG. 3. Signal peptidase cleavage probability in the M28p N-terminus (von Heijne, 1986).

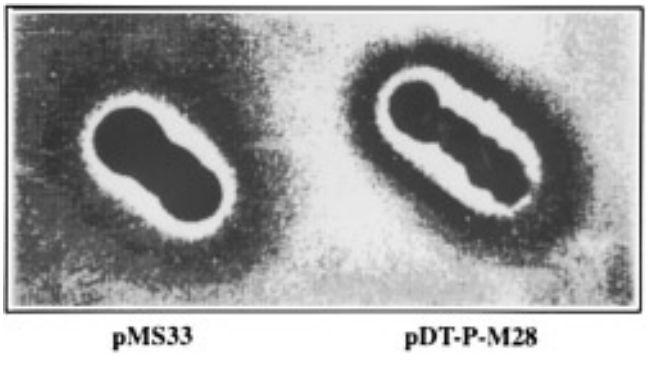

FIG. 4. Killer toxin production of strain GG100-14D transformed with the K28 expression vectors pMS33 and pDT-P-M28. Toxin production was estimated from the size of the zone of growth inhibition of the lawn of the hypersensitive strain 381.

sumably reflects the higher efficiency with which the native signal of M28p functions to direct secretion of M28p into the lumen of the endoplasmic reticulum, consistent with normal initiation of M28p at codon 1.

To allow regulated expression of the K28 phenotype, the p*PGK* promoter fragment in pDT-P-M28 was replaced with the p*GAL1* promoter, producing pDT-G-M28. When transformants were grown in the Gal$^+$ strains GG100-14d or CRY1 on glucose medium, no toxin or immunity was expressed. Toxin levels produced in galactose medium were two- to fourfold higher than for pDT-P-M28p, approaching the level of expression from M28 dsRNA seen in the *ski2* mutant strain MS300c (Schmitt and Tipper, 1992).

Role of Kex2p and Kex1p in K28 killer toxin expression

In vitro analysis of Kex2p protease activity against simple peptides showed it to cut most efficiently after LysArg or ArgArg, with the K_{cat}/K_m for LysArg being 5- to 10-fold higher (Brenner and Fuller, 1992). ProArg was cut with much lower efficiency and other sites, such as AlaArg, with even lower efficiency (Brenner and Fuller, 1992). Cutting after GluArg was not tested. *In vivo,* context would be expected to affect cleavage efficiency, and inspection of known Kex2p processing sites indicates preference for sites with a hydrophobic residue in the P4 position (Tao *et al.,* 1990). Kex2p, therefore, is predicted to cut efficiently after LeuTyrLysArg$_{192}$ and LeuGlnLysArg$_{245}$ in M28p (Fig. 1A). M28p contains no other clearly predicted sites for cleavage by Kex2p.

The role of Kex2p in processing K28 killer toxin was tested by transforming pDT-P-M28 into strains BFY126-35A (*kex2*::*HIS3*) and ME938 (*kex2*::*ura3*), nonkillers lacking M dsRNA. Although transformants of the isogenic Kex$^+$ strains CRY1 and MT960 were normal immune killers and transformants of the *kex2*Δ strains had normal immunity, the latter were completely devoid of secreted toxin activity or protein (data not shown). Following a cross between strain ME938 and the M28 killer strain MS205, the diploid was an immune killer, and all spore progeny maintained M28 dsRNA and were immune. However, toxin secretion and nonsecretion segregated 2:2. It is concluded that *KEX2* function is essential for expression of the K28 killer toxin.

The role of Kex1p was tested by transforming pDT-P-M28 into strains S86-16c (*kex1*::*URA3*) and its Kex$^+$ parent S86c (Cooper and Bussey, 1989). While the Kex$^+$ strain again expressed the complete killer phenotype and immunity was normal in the *kex1* null mutant, toxin expression in the latter was reduced by 80%. We also tested the dependence of the M28 dsRNA encoded killer phenotype on *KEX1* function by crossing strain MS205 to the *kex1* null mutant strain S86-16c (Fig. 5, lanes 1 and 2, respectively). Meiotic segregants were tested for K28 toxin production and immunity. All segregants had normal immunity and M28 dsRNA content (data not shown). As shown in Fig. 5 lanes 3–6, low and normal levels of secreted killer toxin activity segregated 2:2. The weak killers were Leu$^+$ and therefore carried the *kex1*::*LEU2* allele. In conclusion, *KEX1* function is important but not essential for secretion of active K28 killer toxin. Neither Kex1p nor Kex2p activity is required for expression of K28 immunity.

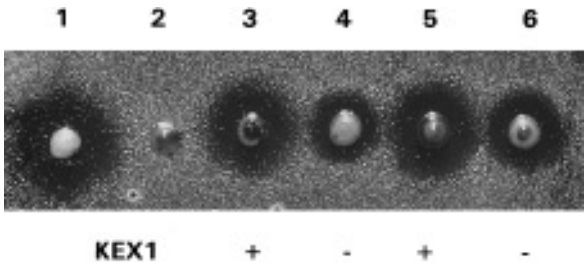

FIG. 5. Toxin killing zones of segregants from cross of the K28 killer strain MS205 (lane 1) to the *kex1* null strain S86-16c (lane 2). The killer phenotype of meiotic segregants from a single tetrad (lanes 3–6) was determined by patching colonies on a pH 4.7 MBA plate seeded with 10^5 cells of the sensitive strain 381. *KEX1* genotype is indicated.

K28 toxin is a nonglycosylated α/β heterodimer

The K28 toxin was previously reported to be a monomeric 16-kDa glycoprotein, serine-rich and carrying O-linked but not N-linked carbohydrate (Schmitt and Pfeiffer, 1990; Pfeiffer and Radler, 1984). However, no plausible fragment of the deduced M28p sequence corresponded to these properties. Toxin preparations, partially purified from culture supernatants of strain 28, were found to contain a minor fraction of about 10 kDa, absent from culture supernatants of its cycloheximide-cured nonkiller derivative 28c, and enriched in affinity-purified toxin preparations (see Materials and Methods). Initial attempts at determining the N-terminal sequence of this fraction suggested that it consisted of at least two protein species. Moreover, the predicted N-glycosylation and Kex2 processing patterns for M28p and M1p are quite similar (see Discussion), suggesting that the mature secreted K28 toxin, like K1 toxin, might be a disulfide-bonded heterodimer. By using 5 to 22% gradient gels, the 11-kDa species was resolved into two species, present in approximately equal amounts (Fig. 6, lane 5). All other K28 killers tested, including K28 virus transfectants of the dsRNA free strain 1938 (Schmitt and Tipper, 1990) and various strains expressing pDT-P-M28, expressed the same pair of proteins, which were absent from the nonkiller parents. The upper component, estimated size 11 kDa, was called β and the lower 10.5-kDa component was called α. This allows the naming of M28p segments to follow the pattern established for M1p (Bostian *et al.,* 1984). N-terminal sequence analysis of α and β produced the sequences underlined in Fig. 1A, precisely reflecting the sequence predicted for M28p and indicating that α and β start at residues 50 and 246, respec-

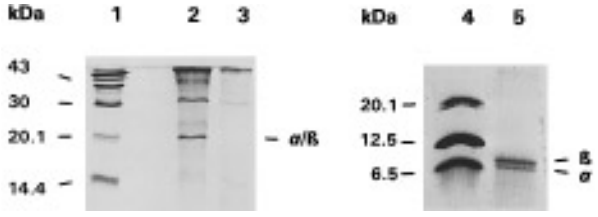

FIG. 6. Gel electrophoretic fractionation of K28 toxin. The sizes of marker proteins (lanes 1 and 4) are indicated. Partially purified toxin was fractionated by SDS–PAGE under nonreducing conditions (15% gel; lane 2) and purified toxin was fractionated in the presence of reducing agent (5–22% gel; lane 5). Lane 3 is a negative control showing a preparation of concentrated, secreted proteins from the cured nonkiller strain 28c.

tively. When the same toxin preparation was fractionated under identical conditions except for the absence of 2-mercaptoethanol (denaturing but nonreducing conditions), a single protein species of about 20 kDa was detected which was absent in the cured, nonkiller strain 28c (Fig. 6, lanes 2 and 3). N-terminal sequence analysis of this 20-kDa species showed a mixture of the α and β components at each position, confirming that it is indeed an α/β heterodimer. Following the nomenclature used for M1p, the segment of M28p between α and β was called γ, and the segment between the presumed signal peptidase cleavage site and the α N-terminus was called δ (Fig. 1D).

The mobilities of α and β and the unreduced α/β heterodimer were unaffected by treatment with endoglycosidase H or by mild alkali hydrolysis, indicating an absence of N- or O-glycosylation. This is also consistent with the absence of staining by carbohydrate reagents and the lack of retention of these toxin components on a concanavalin A–Sepharose column (not shown). The 16-kDa secreted glycoprotein previously identified with K28 toxin (Schmitt and Pfeiffer, 1990) is considerably more abundant than the K28 toxin in supernatants of cultures of strain 28 and was found to copurify with toxin in most other procedures, suggesting that they may interact.

Predictions of M28 RNA plus-strand secondary structure

The yeast L-A dsRNA virus and its M1, M2, and M28 satellites contain only two recognized protein species, capsid and the cap–pol fusion protein. The replication cycle involves at least three RNA sequence recognition events by cap–pol. Within the intact virus, conservative transcription of the plus strand from the parent viral dsRNA requires recognition of its 5′-terminal sequence by the polymerase. In M28 as in the other dsRNAs, the plus strand initiates with GAAAAA. Since there is little if any additional homology immediately downstream (the M2p ORF, for example, follows immediately) (Dignard *et al.,* 1991), this 5′-terminal recognition element (5′-TRE) may be all that is necessary for initiation of transcription. Local secondary structure, however, may be important in initiation of either transcription or translation. Following extrusion of the plus-strand transcript from the virion, cap–pol initiates the next stage of viral replication, encapsidation of its own messenger, the L-A plus strand, and those of the killer satellite viruses (Fujimura *et al.,* 1992). Finally, cap–pol must recognize the 3′-terminus of the encapsidated plus strands in order to initiate minus-strand replication, completing the viral replication cycle (Wickner, 1993). In the following discussion, because both L-A and M dsRNAs give rise to defective-interfering species by deletions that remove most upstream sequence but leave the 3′-sequences intact (Wickner, 1992; Shen and Bruenn, 1993) and since the size of the poly(A) tract in M species is variable (Hannig *et al.,* 1986), positions of internal sequences critical to replication are given relative to the 3′-termini.

Using a gel retardation assay for binding of L-A transcripts to empty viral particles and an *in vivo* encapsidation assay, an RNA stem–loop structure, with a GAUUC loop starting at −391 (i.e., 391 bp from the 3′-terminus), 3 bp downstream of an unpaired (bulged) A, was found to be essential for encapsidation (Fig. 7A) (Fujimura *et al.,* 1990). This structure was called the viral binding site (VBS). Two sequence elements were found to be essential for L-A replication, an internal replication enhancer (IRE), essentially indistinguishable from the VBS, and a small stem–loop structure 5 bp from the 3′-terminus, the 3′-TRE (Fig. 7A) (Wickner, 1993). The M1 sequence contains a very similar VBS/IRE element, with a bulged A and a GAUUC loop starting at −435 (Fig. 7B) (Fujimura *et al.,* 1990). A potential 3′-TRE occurs 23 bp from the 3′-terminus of M1, but the homology is not marked (Fig. 7B). Mutational analysis demonstrated that both the 5 bases of the consensus loop sequence (GAUYC) and the unpaired (bulged) A in its stem were essential for VBS function, while the stem sequence was only necessary to provide secondary structure (Fujimura *et al.,* 1990). A larger fragment of M1, when expressed from the *GAL* promoter, was found to be capable of interfering with the maintenance of M1, presumably by competing for cap–pol (Shen and Bruenn, 1993). The minimal fragment causing curing of M1 included both the VBS and a second similar stem–loop structure with the same GAUUC loop (starting at −379) but with an ACA bulge instead of the single A residue (Fig. 7B). The −379 stem–loop was also shown to have *in vitro* VBS activity; following mutagenic analysis, it was concluded that the consensus VBS element is a GAUYC loop on a 3-base stem separated from a longer stem by either a bulged A or a small bulged loop. The combination of the two VBS elements considerably enhanced interaction with cap–pol, and it was postulated that this enhancement is necessary for the M1 plus strand to compete with L-A plus strand for binding to cap–pol, since L-A has the advantage of acting *in cis* (Shen and Bruenn, 1993).

The M28 sequence contains two potential VBS elements, at −331 and −106 (Fig. 7C). Both have 5-bp loops,

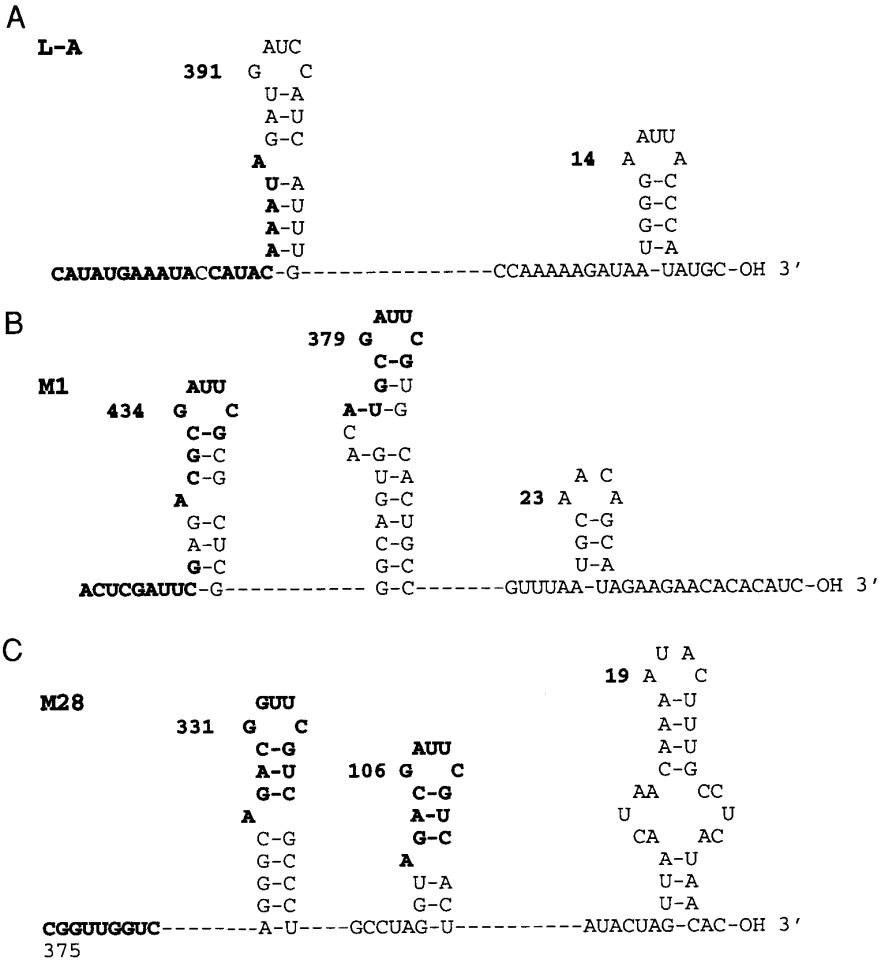

FIG. 7. Comparison of the potential VBS/IRE and 3′-TRE sequence elements in M28 (C) with those in L-A (A) and M1 (B). Numbers are shown for distance from the 3′-terminus of the unpaired A residues which interrupt each VBS stem.

the second identical to that in M1 (GAUUC) and the first differing by 1 base (GGUUC). Each is separated from a bulged A by the identical 3-bp stem, resulting in an 11 of 12-bp repeat (shown in boldface in Figs. 1A and 7C). The last 9 bp of this repeat is reiterated at −375; the first but not the second VBS in M1 also overlaps a 10-bp imperfect direct repeat that includes the VBS loop (in boldface in Fig. 7B). The stem of the L-A VBS also overlaps a direct repeat (Fig. 7A), not including the loop. The significance of these repeats is unknown. Use of the foldrna, mfold, and squiggles algorithms of the GCG sequence analysis program indicated a highly ordered potential secondary structure for the entire 553-base sequence downstream of the poly(A) sequence in the M28 plus strand. Inspection of the 13 most energetically favorable structures shows that all contain the −106 loop with its bulged A at the end of a long stem. The −331 loop was predicted in only 9 of these 13 structures (e.g., Fig. 8). The closest to a match to a 3′-TRE is a weak stem–loop at −19, with scant resemblance to either the M1 or L-A elements (Fig. 7C). This loop, also shown in boldface in Fig. 1A, is predicted by mfold only at the lower energies examined (Fig. 8).

pDT-G-M28b is a YEp multicopy plasmid in which the 693-bp cDNA segment of the M28 plus strand downstream of the M28p gene is transcribed from the *GAL1* promoter. The killer phenotype was stable in pDT-G-M28b transformants of the Gal$^+$ K1 killer strain GGMS1 grown on glucose media but was lost, together with M1 dsRNA, when transformants were grown on galactose medium (not shown). Killer phenotype was stable under these growth conditions in a control transformed with the p21-GAL1-SPB vector. The M28b transcript, which includes the two postulated VBS elements, presumably competes with M1 transcripts for cap–pol, preventing M1 dsRNA replication, as postulated for transcripts of the M1 3′-fragment (Shen and Bruenn, 1993). Thus, the cloned M28 cDNA has at least one of the functional characteristics associated with a satellite of L-A.

DISCUSSION

Cloning of cDNA copies of killer dsRNAs has been notoriously difficult, presumably reflecting the high degree of secondary structure in the separated strands. This is the first complete killer dsRNA sequence re-

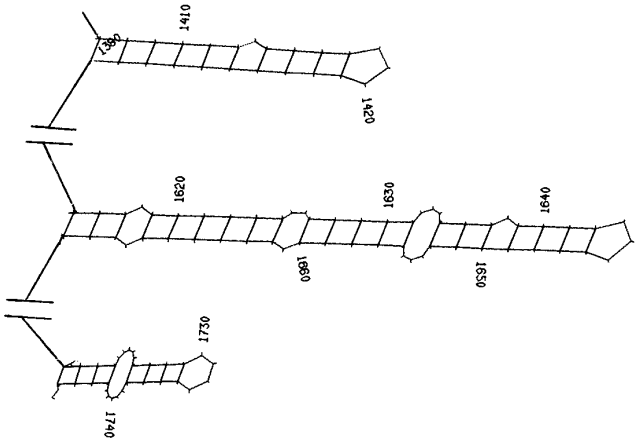

FIG. 8. Segments of the predicted secondary structures of the M28 plus strand, from the end of the poly(A) to the 3′-terminus (bases 1190–1748), drawn using the Squiggle plot of the GCG program. Bases 1417, 1642, and 1730 correspond to bases 331, 106, and 19 from the 3′-end, as indicated in the stem–loops in Fig. 7. The outlying GC residues of the 5-bp loops shown in Fig. 7 are paired here in the 3-bp stem. The stem–loops at 1417 and 1642 were seen at the highest energy (118.5 kcal in *m*fold) and the 1642 stem–loop was seen at all energies tested. The loop at 1417 was seen at only 9 of 13 energies and the weak stem–loop at 1730 was only predicted at 116 kcal, the lowest tested.

ported, although essentially all of the M1 sequence can be deduced from fragmentary data (Bostian *et al.,* 1984; Georgopoulos *et al.,* 1986). Several arguments support the validity of the sequence reported here for the M28 dsRNA. First, its length, 1748 bp, is consistent with the 1.8-kb size estimated for the dsRNA. Second, the predicted sequence of the M28p open reading frame includes the exact terminal sequences of the secreted toxin components and its expression confers the complete K28 killer phenotype on a sensitive cell. Third, the poly(A) stretch in M28 is similar in size and location to that in M1 and the downstream 3′ sequences are of similar size and both contain a pair of predicted VBS/IRE structural elements. The ability of transcripts of this 3′-sequence to interfere with maintenance of M1 is consistent with VBS function (Shen and Bruenn, 1993). The poly(A) stretch is probably of variable length in the parent M28 dsRNA, as in M1 dsRNA (Hannig *et al.,* 1986). These segments resemble the poly(A) tracts in the pseudogenes of higher organisms; however, if they are the residua of reverse transcription events, the absence of any detectable M1p or M28p homolog in the *S. cerevisiae* chromosome is unexplained. Their function may be to allow optimization of the size of M dsRNAs to fit as two copies in a virion built to encapsidate its parent 4.6-kb L-A dsRNA (Wickner, 1993).

The M28p RNA and protein sequences were compared to the latest available DNA and protein data bases using the GCG program and FASTA and TFASTA algorithms. No significant homologies emerged. A search for peptide sequences corresponding to functional segments of known protein families was also fruitless. In K1 toxin the hydrophilic β component is not needed for immunity and is primarily responsible for lectin function in binding of toxin to the cell wall glucan; the α component appears to be primarily responsible for the lethal events of membrane channel formation, probably involving its relatively hydrophobic central segment (Sturley *et al.,* 1986; Zhu *et al.,* 1993). The mechanism of inhibition of DNA synthesis by the K28 toxin, however, is not understood and the sequences of the predicted toxin fragments provide few clues to function; three short stretches in α are hydrophobic (51–61, 78–92, and 121–129), while β is quite hydrophilic. Perhaps the β toxin component in K28 toxin is also responsible for binding to cell wall, allowing α to interact with its hypothetical membrane receptor (Tipper and Schmitt, 1991). Since it seems unlikely that either component of K28 toxin would be able to cross the membrane of an endocytic vesicle to reach the nucleus directly, interaction with a plasma membrane receptor, activating some signal transduction pathway for control of DNA synthesis, seems more likely.

Given the lack of apparent overlap in function of the mature K1 and K28 toxins, the marked conservation of their basic bipartite structure and in the patterns of precursor processing (Fig. 9) are striking. The conservation in processing pattern extends to the internal Kex2p cleavage site and three similarly located N-glycosylation sites in γ (Fig. 9). This conserved pattern may reflect a common strategy for the production of immunity. The γ segment is presumed to function as an internal chaperone for protoxin folding in the ER. It is also presumed to inhibit toxin action so that production of mature, active toxin is delayed until the late Golgi, where Kex2p is active. Immunity to K1 toxin, at least, probably results from nonlethal interaction, earlier in the secretion pathway, of protoxin with the toxin membrane receptor, forming a complex which is directed to and destroyed in the vacuole (Sturley *et al.,* unpublished observations). Premature K1 toxin activation prevents growth (Zhu *et al.,* 1993).

Processing of M28p should initiate with signal peptidase cleavage and N-glycosylation on entry into the endoplasmic reticulum. The reason for the apparent redundancy in signal function is unclear although expression from the first AUG codon is about fourfold more efficient than expression from codon 15, when only the second

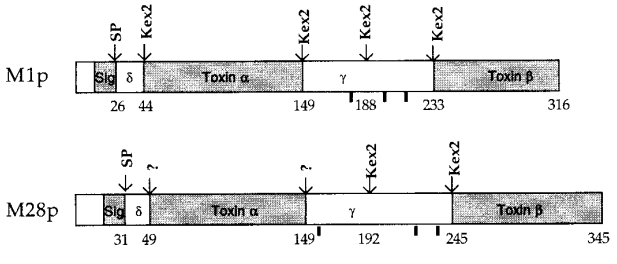

FIG. 9. Comparison of potential processing sites in M1p and M28p. Sites known to be cleaved by Kex2p in M1p and predicted to be cut by Kex2p in M28p are indicated. The site of the α C-terminus in M28p has not been determined; the activities responsible for cleavage at the predicted site and at the α N-terminus are also undetermined.

TABLE 2

Properties of Predicted M28p Preprotoxin Fragments

Residues	Fragment	MW	p*I*	% nonpolar
1–345	Preprotoxin	37,643	4.3	39.6
1–31	Signal A + B	3421	6.1	54.8
32–49	δ	2136	8.8	22
50–149	α toxin	10,706	4.3	45
50–148	α after kex1p	10,549	4.1	45.4
150–245	γ	10,349	4.3	39.6
150–192	γA	4793	3.9	37.3
193–245	γB	5574	6.0	41.6
246–345	β toxin	11,103	4.0	33
246–344	β after kex1p	10,947	3.9	33.3
32–345	Protoxin	34,240	4.3	38.4

Note. Core glycosylation of the three predicted sites in γ should add about 7.5 kDa.

signal is present. M1p has a single clearly defined signal whose cleavage site at Ala_{26} has been verified (Zhu *et al.,* 1992). M2p also has a single easily discernible signal at residues 31–51 (Dignard *et al.,* 1991), so that the redundancy in M28p is unique in known killer preprotoxins. However, a similar signal redundancy is found in the *PHO5* gene (Haguenauer, 1992). Whichever signal actually functions in M28p, additional N-terminal processing is needed to produce the α N-terminus, since signal peptidase cleavage after Gly_{36} becomes highly improbable (Fig. 3). Since the β N-terminus occurs after an optimal Kex2p site, one role for Kex2p in producing the K28 toxin is clear, consistent with the observation that Kex2p function is essential. A 100-residue β fragment would be produced, although this should be reduced to 99 by Kex1p removal of the C-terminal Arg residue. Either product would be consistent with the observed size of β (Table 2). Kex1p is essential for activating K1 toxin, probably for trimming of the α C-terminus (Zhu *et al.,* 1987). Since Kex1p action is important for K28 toxin activity but not for toxin secretion, it is presumably needed to process either the α or β C-terminus. Kex1p action on β would produce a HisAspGluLeu C-terminal ER retention signal. However, since trimming should occur only after translocation from the ER to the late Golgi and ER retention would be inconsistent with toxin secretion, the significance of this sequence is obscure.

The α N-terminus is presumably produced by endoprotease cleavage after $LeuGluGluArg_{49}$, although aminopeptidase action is not excluded. Since α is not glycosylated, it probably terminates before Asn_{161}, whose context suggests facile N-glycosylation. The size of α, deduced from gel mobility, is precisely consistent with cleavage after $IleGlnSerArg_{149}$ (Table 2). Arg_{149} is the only basic residue in the vicinity that might mark a site for cleavage by known processing endoproteases. The product, 100 residues in length, would presumably be reduced to a 99-residue, 10.5-kDa protein by Kex1p action (Table 2). Determination of the α C-terminal sequence will be necessary to test this hypothesis. Neither of the cleavage sites predicted for the α termini resembles the established Kex2p specificity profile. Yap3p is a membrane-anchored aspartyl protease whose overexpression can suppress loss of Kex2p activity (Egel *et al.,* 1990), indicating some overlap in specificity. However, Yap3p is primarily responsible for cleavage after LeuGluArg in presomatostatins expressed in yeast (Bourbonnais *et al.,* 1993). Yap3p may, therefore, play a major role in processing the α component of K28 toxin.

The extensive 3′ noncoding regions in M28 and M1 have no apparent homology to each other or to L-A, other than in the presumed VBS/IRE elements (Fig. 7). The existence of two potential VBS in the M28 plus strand, however, presumably enhances its ability to compete with the L-A transcript for binding to cap–pol, as demonstrated for the ILE fragment of M1 which also contains two VBS (Shen and Bruenn, 1993). In fact, the M28 virus is able to exclude both M1 and M2 viruses during replication in a common host (Schmitt and Tipper, 1992) and presumably is the most efficient in binding cap–pol. Comparison of the L-A, M1, and M28 sequences indicates a consensus cap–pol binding site to be a GRUYC loop on a three-basepair stem separated from a longer stem by a bulged 5′ A residue. We are attempting to reproduce the M28 virus from transcripts of M28 cDNA. If successful, we will be able to test the importance of these sequence elements for replication *in vivo.*

ACKNOWLEDGMENTS

We thank Claudia Darmstadt and Jing Wang for technical assistance. This investigation was supported by Grant Schm 541/3-2 from the DFG to M.J.S. and by Grant VM80 from the American Cancer Society to D.J.T.

REFERENCES

Bostian, K. A., Elliott, Q., Bussey, H., Burn, V., Smith, A., and Tipper, D. J. (1984). Sequence of the preprotoxin dsRNA gene of type I killer yeast: Multiple processing events produce a two-component toxin. *Cell* 36, 741–756.

Bostian, K. A., Jayachandran, S., and Tipper, D. J. (1983). A glycosylated protoxin in killer yeast: Models for its structure and maturation. *Cell* 32, 169–180.

Bourbonnais, Y., Ash, J., Daigle, M., and Thomas, D. Y. (1993). Isolation and characterization of S-cerevisiae mutants defective in somatostatin expression — Cloning and functional role of a yeast gene encoding an aspartyl protease in precursor processing at monobasic cleavage sites. *EMBO J.* 12, 285–294.

Brenner, C., and Fuller, R. S. (1992). Structural and enzymatic characterization of a purified prohormone-processing enzyme — Secreted, soluble Kex2 protease. *Proc. Natl. Acad. Sci. USA* 89, 922–926.

Bussey, H. (1991). K1 killer toxin, a pore-forming protein from yeast. *Mol. Microbiol.* 5, 2339–2343.

Cartwright, C. P., Li, Y., Zhu, Y. S., Kang, Y. S., and Tipper, D. J. (1994). Use of beta-lactamase as a secreted reporter of promoter function in yeast. *Yeast* 10, 497–508.

Cooper, A., and Bussey, H. (1989). Characterization of the yeast KEX1 gene product: A carboxypeptidase involved in processing secreted precursor proteins. *Mol. Cell. Biol.* 9, 2706–2714.

Dignard, D., Whiteway, M., Germain, D., Tessier, D., and Thomas,

D. Y. (1991). Expression in yeast of a cDNA copy of the K2 killer toxin gene. *MGG. Mol. Gen. Genet.* 227, 127–136.

Dinman, J. D., and Wickner, R. B. (1992). Ribosomal frameshifting efficiency and gag/gag-pol ratio are critical for yeast M(1) double-stranded RNA virus propagation. *J. Virol.* 66, 3669–3676.

Dinman, J. D., and Wickner, R. B. (1994). Translational maintenance of frame-mutants of Saccharomyces cerevisiae with altered-1 ribosomal frameshifting efficiencies. *Genetics* 136, 75–86.

Dmochowska, A., Dignard, D., Henning, D., Thomas, D. Y., and Bussey, H. (1987). Yeast KEX1 gene encodes a putative protease with a carboxypeptidase B-like function involved in killer toxin and alpha-factor precursor processing. *Cell* 50, 573–584.

Egel, M. M., Flygenring, H. P., and Hansen, M. T. (1990). A novel aspartyl protease allowing KEX2-independent MF alpha propheromone processing in yeast. *Yeast* 6, 127–137.

Fujimura, T., Esteban, R., Esteban, L. M., and Wickner, R. B. (1990). Portable encapsidation signal of the L-A double-stranded RNA virus of *S. cerevisiae. Cell* 62, 819–828.

Fujimura, T., Ribas, J. C., Makhov, A. M., and Wickner, R. B. (1992). Pol of gag-pol fusion protein required for encapsidation of viral RNA of yeast L-A-virus. *Nature* 359, 746–749.

Georgopoulos, D. E., Hannig, E. M., and Leibowitz, M. J. (1986). Sequence of the M1-2 region of killer virus double-stranded RNA. *Basic Life Sci.* 40, 203–13.

Gietz, R. D., and Schiestl, R. H. (1991). Applications of high efficiency lithium acetate transformation of intact yeast cells using single-stranded nucleic acids as carrier. *Yeast* 7, 253–263.

Haguenauer, T. R. (1992). Protein-specific features of the general secretion pathway in yeast: The secretion of acid phosphatase. *Mol. Microbiol.* 6, 573–579.

Hanes, S. D., Burn, V. E., Sturley, S. L., Tipper, D. J., and Bostian, K. A. (1986). Expression of a cDNA derived from the yeast killer preprotoxin gene: Implications for processing and immunity. *Proc. Natl. Acad. Sci. USA* 83, 1675–1679.

Hannig, E. M., Williams, T. L., and Leibowitz, M. J. (1986). The internal polyadenylate tract of yeast killer virus M1 double-stranded RNA is variable in length. *Virology* 152, 149–158.

Icho, T., and Wickner, R. B. (1989). The double-stranded RNA genome of yeast virus L-A encodes its own putative RNA polymerase by fusing two open reading frames. *J. Biol. Chem.* 264, 6716–6723.

Kang, Y. S., Kane, J., Kurjan, J., Stadel, J. M., and Tipper, D. J. (1990). Effects of expression of mammalian G alpha and hybrid mammalian-yeast G alpha proteins on the yeast pheromone response signal transduction pathway. *Mol. Cell. Biol.* 10, 2582–2590.

Laemmli, U. K. (1970). Cleavage of structural proteins during the assembly of bacteriophage T4. *Nature* 227, 680–685.

Lolle, S., Skipper, N., Bussey, H., and Thomas, D. Y. (1984). The expression of cDNA clones of yeast M1 double-stranded RNA in yeast confers both killer and immunity phenotypes. *EMBO J.* 3, 1383–1387.

Matsudaria, P. (1987). Sequence from picomole quantities of proteins electroblotted onto polyvinylidene difluoride membranes. *J. Biol. Chem.* 262, 10035–10038.

Pfeiffer, P., and Radler, F. (1984). Comparison of the killer toxin of several yeasts and the purification of a toxin of type K2. *Arch. Microbiol.* 137, 357–361.

Sanger, F., Nicklen, S., and Coulson, A. R. (1977). DNA sequencing with chain-terminating inhibitors. *Proc. Natl. Acad. Sci. USA* 74, 5463–5467.

Schmitt, M. J. (1995). Cloning and expression of a cDNA copy of the viral K-28 killer toxin gene in yeast. *Mol. Gen. Genet.* 246, 236–246.

Schmitt, M., Brendel, M., Schwarz, R., and Radler, F. (1989). Inhibition of DNA synthesis in *Saccharomyces cerevisiae* by yeast killer toxin KT28. *J. Gen. Microbiol.* 135, 1529–1535.

Schmitt, M. J., and Pfeiffer, P. C. (1990). Immunochemical analysis of the carbohydrate moiety of yeast killer toxin K28. *Antonie Van Leeuwenhoek* 58, 277–282.

Schmitt, M., and Radler, F. (1987). Mannoprotein of the yeast cell wall as primary receptor for the killer toxin of *Saccharomyces cerevisiae* strain 28. *J. Gen. Microbiol.* 133, 3347–3354.

Schmitt, M., and Radler, F. (1989). Purification of yeast killer toxin KT28 by receptor-mediated affinity chromatography. *J. Chromatogr.* 469, 448–452.

Schmitt, M., and Tipper, D. J. (1990). K_{28}, a unique double-stranded RNA killer virus of *Saccharomyces cerevisiae. Mol. Cell. Biol.* 10, 4807–4815.

Schmitt, M. J., and Tipper, D. J. (1992). Genetic analysis of maintenance and expression of L and M double-stranded RNAs from yeast killer virus-K(28). *Yeast* 8, 373–384.

Shen, Y. Q., and Bruenn, J. A. (1993). RNA structural requirements for RNA binding, replication, and packaging in the yeast double-stranded RNA virus. *Virology* 195, 481–491.

Skipper, N. (1983). Synthesis of a double-stranded cDNA transcript of the killer toxin-coding region of the yeast M1 double-stranded RNA. *Biochem. Biophys. Res. Commun.* 114, 518–525.

Steiner, D. F., Smeekens, S. P., Ohagi, S., and Chan, S. J. (1992). The new enzymology of precursor processing endoproteases. *J. Biol. Chem.* 267, 23435–23438.

Sturley, S. L., Elliot, Q., LeVitre, J., Tipper, D. J., and Bostian, K. A. (1986). Mapping of functional domains within the Saccharomyces cerevisiae type 1 killer preprotoxin. *EMBO J.* 5, 3381–3389.

Tao, J., Ginsberg, I., Banerjee, N., Held, W., Koltin, Y., and Bruenn, J. A. (1990). Ustilago maydis KP6 killer toxin: Structure, expression in Saccharomyces cerevisiae, and relationship to other cellular toxins. *Mol. Cell. Biol.* 10, 1373–1381.

Tipper, D. J., and Schmitt, M. J. (1991). Yeast dsRNA viruses: Replication and killer phenotypes. *Mol. Microbiol.* 5, 2331–2338.

von Heijne, G. (1986). A new method for predicting signal sequence cleavage sites. *Nucleic Acids Res.* 14, 4683–4690.

Wickner, R. B. (1992). Double-stranded and single-stranded RNA viruses of Saccharomyces cerevisiae. *Annu. Rev. Microbiol.* 46, 347–375.

Wickner, R. B. (1993). Double-stranded RNA virus replication and packaging. *J. Biol. Chem.* 268, 3797–3800.

Wickner, R. B., and Leibowitz, M. J. (1976). Two chromosomal genes required for killing expression in killer strains of Saccharomyces cerevisiae. *Genetics* 82, 429–442.

Zhang, H. Y., Komano, H., Fuller, R. S., Gandy, S. E., and Frail, D. E. (1994). Proteolytic processing and secretion of human beta-amyloid precursor protein in yeast — Evidence for a yeast secretase activity. *J. Biol. Chem.* 269, 27799–27802.

Zhu, H., Bussey, H., Thomas, D. Y., Gagnon, J., and Bell, A. W. (1987). Determination of the carboxyl termini of the alpha and beta subunits of yeast K1 killer toxin. Requirement of a carboxypeptidase B-like activity for maturation. *J. Biol. Chem.* 262, 10728–10732.

Zhu, Y. S., Kane, J., Zhang, X. Y., Zhang, M., and Tipper, D. J. (1993). Role of the gamma-component of preprotoxin in expression of the yeast K(1) killer phenotype. *Yeast* 9, 251–266.

Zhu, Y. S., Zhang, X. Y., Cartwright, C. P., and Tipper, D. J. (1992). Kex2-dependent processing of yeast K1 killer preprotoxin includes cleavage at ProArg-44. *Mol. Microbiol.* 6, 511–520.